Global Change Biology (2004) **10,** 718–730, doi: 10.1111/j.1529-8817.2003.00762.x

Effects of an experimental drought on soil emissions of carbon dioxide, methane, nitrous oxide, and nitric oxide in a moist tropical forest

ERIC A. DAVIDSON*, FRANÇOISE YOKO ISHIDA† and DANIEL C. NEPSTAD*
The Woods Hole Research Center, PO Box 296, Woods Hole, MA 02543, USA, †Instituto de Pesquisa Ambiental da Amazônia, Av. Nazaré, 669-Belém, PA 66035-170, Brazil

Abstract

Changes in precipitation in the Amazon Basin resulting from regional deforestation, global warming, and El Niño events may affect emissions of carbon dioxide (CO_2), methane (CH_4), nitrous oxide (N_2O), and nitric oxide (NO) from soils. Changes in soil emissions of radiatively important gases could have feedback implications for regional and global climates. Here we report results of a large-scale (1 ha) throughfall exclusion experiment conducted in a mature evergreen forest near Santarém, Brazil. The exclusion manipulation lowered annual N_2O emissions by $>40\%$ and increased rates of consumption of atmospheric CH_4 by a factor of >4. No treatment effect has yet been detected for NO and CO_2 fluxes. The responses of these microbial processes after three rainy seasons of the exclusion treatment are characteristic of a direct effect of soil aeration on denitrification, methanogenesis, and methanotrophy. An anticipated second phase response, in which drought-induced plant mortality is followed by increased mineralization of C and N substrates from dead fine roots and by increased foraging of termites on dead coarse roots, has not yet been detected. Analyses of depth profiles of N_2O and CO_2 concentrations with a diffusivity model revealed that the top 25 cm soil is the site of most of the wet season production of N_2O, whereas significant CO_2 production occurs down to 100 cm in both seasons, and small production of CO_2 occurs to at least 1100 cm depth. The diffusivity-based estimates of CO_2 production as a function of depth were strongly correlated with fine root biomass, indicating that trends in belowground C allocation may be inferred from monitoring and modeling profiles of H_2O and CO_2.

Key words: Amazon Basin, Brazil, CH_4, climate change, CO_2, N_2O, nitrogen, NO, soil carbon

Received 1 November 2002; revised version received and accepted 1 May 2003

Introduction

Regional climate in the Amazon Basin may become drier as a result of less recirculation of water between the deforested biosphere and the atmosphere (Shukla *et al*., 1990; Nobre *et al*., 1991; Costa & Foley, 2000; Werth & Avisar, 2002). Global warming may also increase the frequency and intensity of El Niño events (Trenberth & Hoar, 1997; Timmermann *et al*., 1999), which cause severe drought in the eastern Amazon Basin (Nepstad *et al*., 1999). Tropical rainfall inhibition by smoke (Rosenfeld, 1999; Andreae *et al*., 2004) may exacerbate this general drying trend in this moist tropical forest region.

Recent rapid land-use change in the Amazon Basin is altering C and N cycles directly (Verchot *et al*., 1999; Dias-Filho *et al*., 2001; Houghton *et al*., 2001). Changes in precipitation could also affect emissions of carbon dioxide (CO_2), methane (CH_4), nitrous oxide (N_2O), and nitric oxide (NO) from the remaining forested soils. Reduced precipitation may have important feedback effects on climate change by altering soil emissions of radiatively important gases, such as CO_2, CH_4, N_2O (Prather *et al*., 1995), and NO (NO is not, itself, a greenhouse gas, but it is a precursor to the formation of tropospheric ozone, which is a greenhouse gas; Lammel

Correspondence: Eric A. Davidson, The Woods Hole Research Center, P.O. Box 296, Woods Hole, MA 02543, USA,
tel. +1 508 540 9900; fax +1 508 540 9700,
e-mail: edavidson@whrc.org

& Graßl, 1995). Upland forest soils of the tropics are known to be important sources of N_2O (Matson & Vitousek, 1990) and NO (Davidson & Kingerlee, 1997) and sinks for CH_4 (Potter *et al*., 1996). Both primary productivity and respiration are high in many tropical ecosystems, resulting in large emissions of CO_2 from soils (Davidson *et al*., 2000b). The direct effects of land-use change in the Amazon region on soil emissions of these gases have been studied (Matson *et al*., 1990; Fearnside 1996; Steudler *et al*., 1996; Verchot *et al*., 1999, 2000; Davidson *et al*., 2000b; Kirkman *et al*., 2002), but the possible effects of changes in precipitation have been addressed only in a single small-scale ($100\,m^2$) pilot experiment (Cattânio *et al*., 2002).

Trace gas emissions are affected by precipitation in at least two ways (Davidson & Schimel, 1995; Davidson *et al*., 2000a): (1) soil water content affects soil aeration, which, in turn, affects microbial processes of production and consumption of these trace gases and (2) reduced precipitation could alter root turnover, litterfall, decomposition, and mineralization, which would, in turn, affect the availability of carbon and nitrogen substrates for trace gas production. However, an increase in available N or C in the soil may first require a change in C allocation by plants, root mortality, or soil faunal activity.

We report here the results of a large-scale (1 ha) throughfall experiment manipulation conducted in the Tapajós National Forest, near Santarém, Pará, Brazil (Nepstad *et al*., 2002). We hypothesized that throughfall exclusion would affect trace gas emissions in two phases. The first phase would be characterized by immediate and direct responses to soil drying, such as increased soil consumption of atmospheric CH_4 due to higher diffusivity in dry soil (Dörr *et al*., 1993; Striegl, 1993), and an increase in the ratio of $NO:N_2O$ produced by nitrification and denitrification in drier soils (Firestone & Davidson, 1989; Davidson *et al*., 2000a). A second phase, which would begin only after drought stress caused significant root mortality, would be characterized by increased substrate availability that would increase emissions of NO, N_2O, and CH_4 due to mineralization of N-rich fine root tissues and enhanced termite foraging on dead coarse roots (Cattânio *et al*., 2002). It is more difficult to predict responses of soil CO_2 emissions because root mortality would both decrease root respiration and possibly increase decomposition of dead roots.

In addition to the overall responses of emissions from the soil surface, we are investigating the effects of throughfall exclusion on the depths within the soil profile where these gases are produced and consumed. Evergreen forests of the eastern Amazon Basin depend upon deep roots to obtain water from 8 m or greater depths through the long dry season (Nepstad *et al*., 1994). Experimentally imposed drought could cause an increase in allocation of C to deep roots. If changes in C allocation are substantial, we would expect to see greater production of CO_2 at depth under the drought stressed treatment. Our surface flux measurements were accompanied by measurements of gases throughout the soil profile, from 10 to 1100 cm depths. We then applied a model of soil diffusivity, based on measures of porosity, water-holding properties, and water content, to calculate the flux of CO_2 and N_2O as a function of soil depth.

Materials and methods

Study area

The Tapajós National Forest, located in east-central Amazonia (2.8968°S, 54.9519°W), receives 600–3000 mm of rain each year, with a mean of 2000 mm, most of which falls during the wet season from January to June (Fig. 1e). El Niño events cause severe droughts (Nepstad *et al*., 1999). The forest is situated on a terrace of tertiary sediments capped by the Belterra Clay Formation (Clapperton, 1993). The Oxisol soil (Haplustox) is acidic (pH 4–5), is dominated by kaolinite clay minerals (60–80% clay), and is free of hardpan or iron oxide concretions in the upper 12 m; the water table is more than 100 m deep. The forest has emergent trees up to 55 m in height, with a continuous canopy at approximately 30 m. Of the trees and lianas ≥ 10 cm diameter at breast height, aboveground biomasses were 348 and 235 $Mg\,ha^{-1}$ in the treatment and control plots, respectively, and the number of species were 169 and 188, respectively (Nepstad *et al*., 2002).

Experimental design

Two 1 ha plots were identified from an initial survey of 20 ha of forest. Details of site selection, research infrastructure, and the broad array of ongoing ecological measurements are available in Nepstad *et al*. (2002). A 1.5 m deep trench was excavated around the perimeter of the treatment plot, to reduce the potential for lateral movement of soil water from the surrounding forest into the plot. A similar trench was excavated around the control plot to avoid the confounding of throughfall exclusion and trenching effects. All measurements reported here were taken at least 20 m from the trench edge to guard against edge effects.

As with many large-scale ecosystem manipulations, this experiment is prohibitively large and expensive to permit replication. Following the successful study

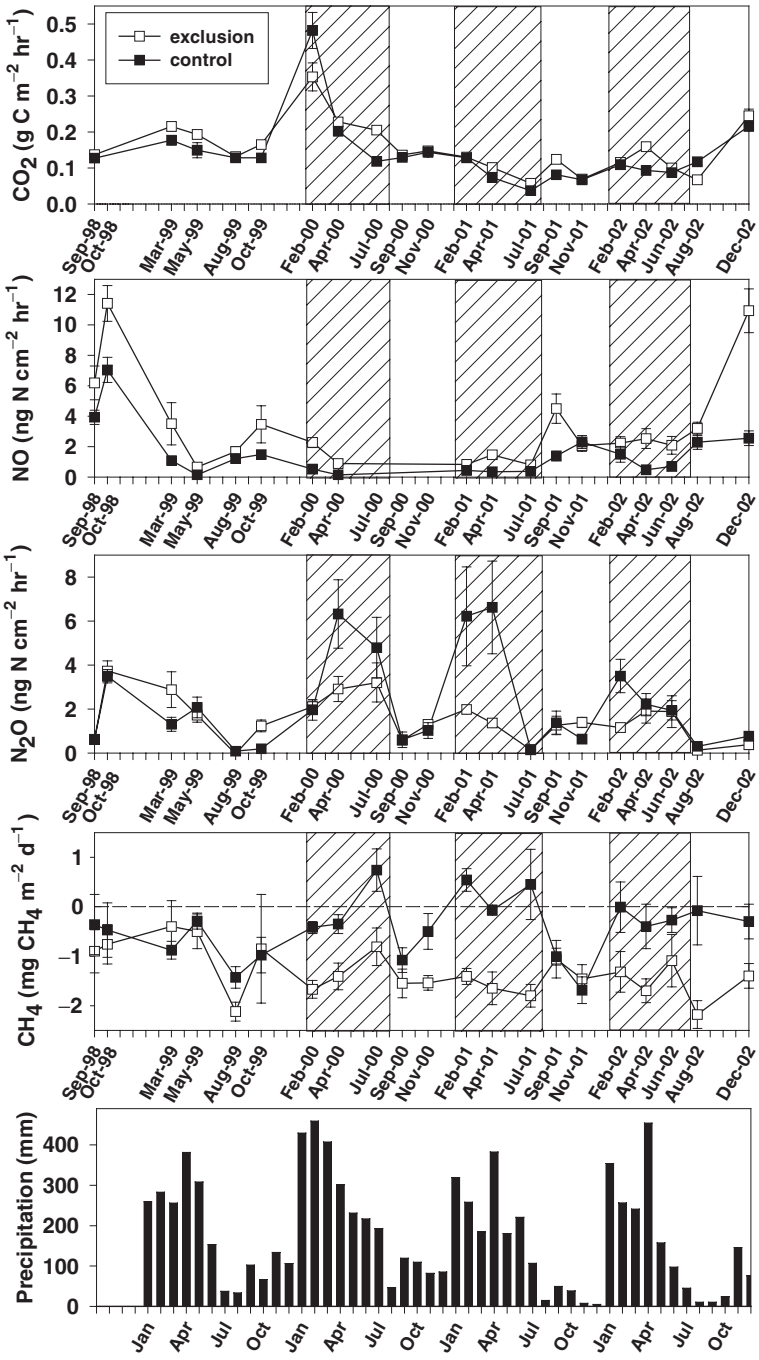

Fig. 1 Monthly mean surface fluxes ($N = 18$) of carbon dioxide, nitric oxide, nitrous oxide, and methane in the throughfall exclusion plot (open symbols) and control plot (solid symbols). For CH_4, negative fluxes indicate net consumption by the soil of atmospheric CH_4, whereas positive values indicate net emission from the soil. The error bars (a few of which are smaller than the plotting symbols) represent standard errors of the mean. Missing data are due to equipment failure. The shaded regions show the periods when the throughfall exclusion panels were in place. Monthly precipitation at the study site for 1999–2002 is shown in the bottom panel.

design of large-scale ecosystem manipulation experiments, such as those at Hubbard Brook, we have intercalibrated the two Amazon plots by making measurements in each plot during an 18-month intercalibration period, beginning in September 1998. By determining differences between the two plots before and after rainfall exclusion, treatment effects are clearly identified as trends of pretreatment similarities and

differences between plots begin to diverge after the treatment begins.

Throughfall was partially excluded from the treatment plot during the rainy season of 2000, from early February through early August, using 5660 panels made of clear, photosynthetically active radiation-transmitting greenhouse plastic mounted on wooden frames. The panels are removed during the dry season to reduce their influence on the forest floor. They were put back in place during the rainy seasons of 2001 and 2002. Only $\sim$1% of solar radiation penetrates the forest canopy (Nepstad *et al*., 1996), and panels change forest floor temperature by $<0.2\,^{\circ}C$. While they are in place, the panels are flipped on their sides every 2 days to transfer accumulated litter onto the forest floor beneath. Each 3 m $\times$ 0.5 m panel drains into a plastic-lined, wooden gutter that carries the water into the trench, which is also lined with plastic; the gutters serve as catwalks for various measurements and panel maintenance. Water flows by gravity from the trenches into a deeper drainage ditch, and into a small valley 250 m away from the plot. The panels and gutters cover only 78% of the forest floor, because we left openings around tree stems. We do not exclude stemflow from the plot, given its small contribution to forest floor soil water input (1–2%, Jipp *et al*., unpublished manuscript), and its disproportionately high contribution to nutrient inputs to the soil. Water yield from the gutters that drain the plot is 72–75% of throughfall, and 58–61% of total rainfall (Nepstad *et al*., 2002).

Root biomass

Soil shafts (12 m deep, with 2.1 m $\times$ 0.8 m openings, $n = 3$ per plot), with a wooden infrastructure, were dug to provide belowground access. Coarse root biomasses to 12 m depth (>2 mm diameter, live and dead) were 33 and 30 Mg ha^{-1} for the treatment and control plots, respectively, based on roots encountered during the excavation of three soil shafts per plot and dried to 65 °C (Table 1). Fine root biomass (0–2 mm diameter, live and dead) was 3.4 and 4.2 Mg ha^{-1} for the treatment and control plots, respectively, based on 20 auger borings to 6 m depth, with 1.5 kg soil samples collected at 0–0.1, 0.5, 1 m, and at 1 m intervals to 6 m depth. Roots were separated from the soil using a combination of sieving of the soil in suspension through a 0.6 mm nylon mesh, and visual inspection of the soil slurry following sieving. Live and dead roots were distinguished using a dissecting scope ($\times$ 10) on the basis of visual criteria and staining, although only total root biomass is reported here.

Table 1 Mean annual trace gas emissions based on 14 sampling dates during the 3 years after initiation of the throughfall exclusion treatment (see text)

	Exclusion	Control
CO_2 (Mg C ha^{-1})	11.8 $\pm$ 1.0	10.0 $\pm$ 0.9
NO (kg N ha^{-1})	2.2 $\pm$ 0.5	0.9 $\pm$ 0.2
N_2O (kg N ha^{-1})	1.5 $\pm$ 0.2	2.6 $\pm$ 1.0
CH_4 (kg CH_4 ha^{-1})	-5.3 ± 1.0	-1.1 ± 1.0

The error terms represent the 95% confidence interval derived from analysis of spatial heterogeneity among the 18 flux chambers per study plot. Note that differences in CO_2 and NO fluxes between treatments are similar to pre-existing differences between plots, whereas differences for N_2O and CH_4 appeared only after the throughfall exclusion treatment began.

Volumetric water content

Volumetric soil water content (VWC; cm^3 water cm^{-3} soil) was measured to 11 m depth in each of the soil shafts using time domain reflectrometry (TDR). The rods of each sensor were imbedded at one end in an epoxy resin head. Each sensor was installed at the end of a 1.5 m auger hole drilled horizontally into the wall of the shaft (the rods pushed into the intact soil) to avoid shaft effects on soil moisture; the holes were then back-filled with soil. Each of the six shafts (three per plot) have duplicate vertical sensors at the soil surface and duplicate horizontal sensors in opposite walls at 50, 100, 200, 300 cm, and at 100 cm intervals to 1100 cm depth. The dielectric constant of the TDR probes was measured with a cable tester, and VWC was estimated from the calibration equation developed in a similar Belterra clay formation, in eastern Amazonia (Jipp *et al*., 1998). The mean VWC was calculated from the duplicate TDR probes at each depth in each shaft.

Soil gases

Fluxes of gases at the soil surface were made using chambers consisting of a polyvinyl chloride (PVC) ring (20 cm diameter $\times$ 10 cm height) and a vented PVC cover made from an end-cap of a 20 cm diameter PVC pipe. In September 1998, PVC rings were pushed into the soil to a depth of 2–3 cm to make the base of the chamber and have been left in place for the duration of the study. Six rings were placed in each of three subplots within the rainfall exclusion plot and the control plots, yielding a sample size of 18 for each treatment.

A dynamic chamber method was used for measuring fluxes of NO (Verchot *et al*., 1999) and CO_2 (Davidson *et al*., 2002). Air drawn from the chamber was circulated

through a Nafion gas sample dryer, a Scintrex LMA-3 NO_2 analyzer (Scintrex Limited, Concord Ont., Canada), and a LiCor infrared gas analyzer (LiCor, Lincoln, NE, USA), and then back to the chamber, using Teflon tubing and a battery operated pump, at a flow rate of $0.5\,L\,min^{-1}$. Varying the flow rate from 0.4 to $1.2\,L\,min^{-1}$ had no detectable effect on measured flux rates. NO is converted to NO_2 by a CrO_3 converter, and the NO_2 is detected by chemiluminescent reaction with Luminol. Fluxes were calculated from the rate of increase of NO and CO_2 concentrations, recorded by a datalogger at 12 s intervals between 1 and 3 min after placing the cover over the ring. The instruments were calibrated twice daily in the field.

Fluxes of N_2O and CH_4 were measured using a static chamber technique (Matson *et al.*, 1990; Verchot *et al.*, 1999, 2000) and using the same chamber bases as those described above. Syringe samples removed from the chamber headspace at 30 s, 10, 20, and 30 min were analyzed in the laboratory by gas chromatography within 48 h, using an electron capture detector (ECD) for N_2O analysis and a flame ionization detector (FID) for CH_4 analysis (Verchot *et al.*, 1999, 2000). Fluxes were calculated from the rate of concentration change, determined by linear regression.

Both dynamic and static chamber flux measurements were made on the same day and, in most cases, within 90 min of each other. Detailed discussion of spatial and temporal variation using this sampling scheme have been addressed in other publications (Verchot *et al.*, 1999, 2000; Davidson *et al.*, 2000b). Fluxes have been measured about five times per year since installation of the rings in 1998, and these measurements are ongoing at the time of this writing.

Stainless steel gas sampling tubes (3 mm diameter) were installed into the walls of each of the six soil shafts at depths of 10, 25, 50, 100, 200, 300, 700, and 1100 cm, following the methodology of Davidson & Trumbore, (1995). The tubes were placed into 1.5 m long horizontal auger holes that were then backfilled. Duplicate gas samples of 20 mL were withdrawn from each tube through a septum and fitting on the exposed end in the soil pit using a nylon syringe. The N_2O and CH_4 concentrations were analyzed by ECD and FID gas chromatography, as described above for syringe samples. The CO_2 concentrations in the soil profiles were sufficiently high that quantification could be achieved with the ECD despite its relatively poor sensitivity to CO_2. Profiles of NO concentrations were not measured.

Soil bulk density and water holding properties

Intact soil cores were collected from 50 cm and at every 100 cm interval between 100 and 1100 cm in shafts 1 and 2 (exclusion plots) and 4 and 5 (control plots). Water retention curves of these intact soil cores were determined on pressure plates by Dr E. J. M. Carvalho in the soil physics laboratory of Embrapa Amazônia Oriental in Belém, Brazil. Data from the water retention curves were used to estimate the parameters needed for the diffusivity model described below. Bulk density was then estimated from the oven-dried soils of these intact cores. Mean bulk densities were 1.0, 1.1, and $1.2\,g\,cm^{-3}$ at the 50, 100–400, and 500–1100 cm depths, respectively.

Modeling effective diffusivity and fluxes of CO_2 and N_2O

Ambient air-filled porosity (ε) was estimated from the difference between total porosity and VWC determined by TDR measurements. Total porosity was calculated from measures of bulk density:

$$\text{Total porosity} = 1 - (\text{DBD}/\text{PD}),$$

where BD is measured bulk density and PD is an assumed particle density of $2.6\,g\,cm^{-3}$. Total porosity was $0.62\,cm^3\,cm^{-3}$ at 50 cm and decreased with depth until about 600 cm depth, where it averaged $0.52\,cm^3\,cm^{-3}$.

The water retention and bulk density data from the cores at 50 cm depth were used for the top 50 cm soil, which may have caused underestimation of diffusivity in the top 25 cm. Because bulk density and water retention curves were measured for soils of only two of the three shafts per treatment, the estimates of total porosity, ε_{100}, and b (see below) for the third shaft were estimated by the means of these values for each depth from the other two shafts.

The ratio of diffusivity in soil (D_P) to diffusivity in air ($D_O = 0.16\,cm^2\,s^{-1}$ for CO_2 and N_2O at 25 °C and 1 atm) was calculated following the model of Moldrup *et al.* (2000):

$$D_P/D_O = (2\varepsilon_{100}^3 + 0.04\varepsilon_{100}) \times (\varepsilon/\varepsilon_{100})^{2+3b},$$

where ε is ambient air-filled porosity (total porosity − VWC), ε_{100} is air-filled porosity at −100 cm H_2O tension (i.e. the −10 kPa treatment of an intact soil core on a pressure plate), and b is the slope of the line determined from the water retention curve:

$$\text{Log} - \Psi = a + b\theta,$$

where Ψ is the water potential and θ is the VWC of the pressure plate measurements. The ε_{100} term represents macroporosity, while the b term characterizes the pore-size distribution, generally increasing with clay content (Moldrup *et al.*, 2000). The mean ε_{100} values declined gradually from $0.27\,cm^3\,cm^{-3}$ at 50 cm depth to $0.06\,cm^3\,cm^{-3}$ at 1100 cm depth. The b values for this clayey soil ranged from 14 near the surface to as high as

35 at depth, but most values were between 20 and 30. Effective diffusivities generally ranged between 0.01 and 0.02 cm^3 air cm^{-1} soil s^{-1} in the top 50 cm and were as low as 0.002 cm^3 air cm^{-1} soil s^{-1} in the deep soil.

Fluxes of CO_2 and N_2O were estimated at each sampling depth by applying Fick's first law:

$$\text{Flux} = D_P \times dC/dz,$$

where D_P is the effective diffusivity calculated as described above and dC/dz is the concentration (C) gradient over depth z. For the flux at 10 cm depth, the gradient between the concentrations at 10 cm and the ambient atmosphere was used. For the flux at 25 cm, the gradient between 25 and 10 cm was used, and so on, for each of the depths to 1100 cm where gas concentrations were sampled. This approach assumes that the concentration profile is momentarily at steady state and that no production or consumption of the gas occurs between the two depth intervals, which are simplifying assumptions that are likely not to be strictly true. However, the approach of Davidson & Trumbore (1995), where an instantaneous flux gradient was calculated at each depth from the tangent of an exponential fit to the concentration profile, was not possible here because the concentration profiles usually did not follow an exponentially increasing concentration with depth. Hence, calculating a concentration gradient for each measured depth increment was judged to be most appropriate. Although there remains uncertainty regarding the magnitude of each individual flux estimate, our objective is to identify the relative trends of gas production as a function of soil depth, season, and treatment, which this approach provides. Where gas concentrations increase with depth, the flux calculated for a given depth using this model provides an estimate of the production that occurred below that depth.

Statistical analyses

The surface gas flux measurements were not normally distributed, so the data were logarithmically transformed prior to analysis of variance. In the case of CH_4 and N_2O, where negative fluxes were observed, an integer (5 CH_4 and 2 for N_2O) was added to all fluxes to make the values positive prior to logarithmic transformations.

A repeated measures design was first used to test differences between the two study plots in 1999, before the throughfall exclusion experiment began. The effect of sample date (repeated measures) was used to determine the effect of seasonality within each plot. Another repeated measures design was used to test the effect of the rainfall exclusion treatment, in which data from one date in the dry season and one date in the wet season in each of the 3 years of post-treatment measurements were included as dependent variables. Year and season were considered as two repeated trial factors. To test the effect of throughfall exclusion on the seasonality of gas fluxes, we examined the interaction of the throughfall exclusion treatment and the repeated measurements across seasons within each year.

Annual estimates of trace gas fluxes were first made for each individual flux chamber. Because there were equal numbers of wet and dry season sampling dates and because the wet and dry seasons are each about 6 months, no special weighting of the data was needed. The average of the fluxes across the 14 post-treatment sampling dates over 3 years was extrapolated to an annual rate. Because there were no more than five sample dates in any year, sampling was not sufficiently frequent to address interannual variation, so the data are combined across all post-treatment years to calculate an average annual flux. After calculating an annual flux for each chamber, the mean and 95% confidence interval was calculated for the 18 chambers within each treatment plot. Hence, temporal variation was addressed in the repeated measures analysis, while the error terms of the annual estimates reflect only spatial heterogeneity.

Results and discussion

Emissions from the soil surface

Fluxes of CO_2 and NO were significantly higher ($P < 0.01$) in the treatment plot than in the control plot in 1998 and 1999, prior to initiation of the throughfall exclusion treatment (Fig. 1a, b). We do not know the reason for this pre-existing difference between plots. These differences persisted at similar amounts throughout the post-treatment period ($P < 0.01$). Therefore, we conclude that there has been no detectable effect of the throughfall exclusion treatment on these two gases. Fluxes of CO_2 were significantly higher and NO fluxes significantly lower during the wet season compared with the dry season ($P < 0.01$), but the interaction of season and throughfall exclusion treatment was not significant ($P > 0.05$).

In contrast, fluxes of N_2O were marginally significantly higher ($P = 0.04$) in the exclusion plot prior to the start of the exclusion treatment, and then became significantly lower in the exclusion plot compared with the control plot ($P < 0.01$) during the wet seasons after the throughfall exclusion began (Fig. 1c). Fluxes of CH_4 were not significantly different ($P > 0.05$) in exclusion and treatment plots prior to the start of the exclusion

treatment, but diverged significantly ($P = 0.01$) after the throughfall exclusion began (Fig. 1d). The effect of season was significant ($P < 0.01$) both before and after the exclusion treatment began for both N_2O and CH_4, and the interaction of treatment and season became significant ($P < 0.01$) for CH_4 only after the treatment began. As expected, fluxes of N_2O were generally higher during the wet season (January–June) than the dry season, but the seasonal variation was diminished in the throughfall exclusion plots (Fig. 1c). Fluxes of CH_4 were negative during the dry season, indicating net consumption of atmospheric CH_4 by the soil (Fig. 1d). During the very wet rainy seasons of 2000 and 2001, net production of CH_4 (positive flux) was occasionally observed in the control plot receiving natural throughfall, whereas the negative fluxes characteristic of the dry season persisted throughout the wet seasons in the exclusion plot.

Nepstad *et al*. (2002) calculated that the throughfall exclusion resulted in a depletion of 100 and 140 mm water storage in the top 2 m of soil in the exclusion plot relative to the control in 2000 and 2001, respectively. We conclude that drier soil conditions caused by throughfall exclusion inhibited N_2O and CH_4 production and promoted CH_4 consumption.

No relationship between VWC of the top 30 cm soil and CO_2 flux was observed (Fig. 2a), except perhaps a weak indication of the highest fluxes at intermediate water contents. The use of matric potential or water-filled pore space as the scalar for water content did not improve this relationship. An unusually large pulse of CO_2 was observed in February 2000, when our sampling happened to follow immediately after a large rainfall event (Fig. 1a). In contrast to CO_2, NO fluxes were negatively correlated with VWC, and N_2O and CH_4 fluxes were positively correlated with VWC (Fig. 2b–d). The ratio of N_2O : NO fluxes was also positively correlated with VWC. Similar results have been shown for many sites, where wet conditions favor the more reduced gas, N_2O, and dry conditions favor the more oxidized gas, NO (Firestone & Davidson, 1989; Davidson *et al*., 2000a; Davidson & Verchot, 2000). Production of CH_4 is enhanced by increased frequency of anaerobic microsites in wet soil, whereas CH_4 consumption is favored in drier soil conditions (Davidson & Schimel, 1995). The effective diffusivity of gases in the soil increases as the soil dries, thus promoting diffusion of atmospheric CH_4 and O_2 into the soil, which can be limiting factors for CH_4 oxidation (Dörr *et al*., 1993; Striegl, 1993; Keller & Reiners, 1994; Verchot *et al*., 2000). The graphs in Fig. 2 demonstrate that the exclusion treatments shifted the VWC toward the drier end of the gradient, thus increasing CH_4 consumption and decreasing production of N_2O and CH_4.

The annual emissions of NO, N_2O, and CH_4 from the control plot (Table 1) are within the ranges reported by other investigators working in Amazonian forests (see review of NO and N_2O by Davidson *et al*. (2001), and review of CH_4 by Verchot *et al*. (2000)). The CO_2 emissions from this site are considerably lower than those measured by Davidson *et al*. (2000b) in a mature forest near Paragominas, Pará, for which there is no obvious explanation.

The annual NO emissions from the exclusion plot were more than double those of the control plot. For reasons that we cannot identify, however, NO emissions had also been higher in the control prior to the exclusion treatment, so this difference cannot be attributed to the throughfall exclusion. For N_2O, on the other hand, the annual emissions from the exclusion plot were about half those of the control plot, and this is a statistically significant effect of the treatment. Similarly, annual rates of consumption of atmospheric CH_4 by the soil were >4 times higher as a result of throughfall exclusion.

We hypothesized that the first phase of response to throughfall exclusion would be the direct effect of soil water content and aeration on soil microbial processes of NO, N_2O, and CH_4 production and consumption. Indeed, this response was observed for N_2O and CH_4 during the first three post-treatment wet seasons. We have not yet observed any indication of a hypothesized second phase response related to substrate availability. If fine root mortality had increased net N mineralization, we would have expected to see elevated NO and N_2O fluxes in the exclusion plot in both dry and wet seasons due to increased N substrate availability, as was observed 3 years after the initiation of the exclusion treatment in a pilot study (Cattânio *et al*., 2002). Likewise, if root mortality had resulted in a larger mass of coarse dead roots for termite foraging, we would have expected increased emissions of CH_4 even in the dry soil (Cattânio *et al*., 2002). Nepstad *et al*. (2002) reported evidence of reduced aboveground net primary productivity and stem wood increment growth in the exclusion plot near the end of the second year of rainfall exclusion. Since then, mortality of understory trees has become apparent and canopy openness has increased in the exclusion plots (Nepstad, unpublished data), indicating that the effects of drought on mortality and C allocation are just now becoming clear. We anticipate that the hypothesized second phase of responses of traces gases will follow in the coming years.

Depth profiles of gas concentrations, VWC, and production estimates

Depth profiles of VWC, CO_2 concentrations, and N_2O concentrations are shown in Fig. 3 for five representative

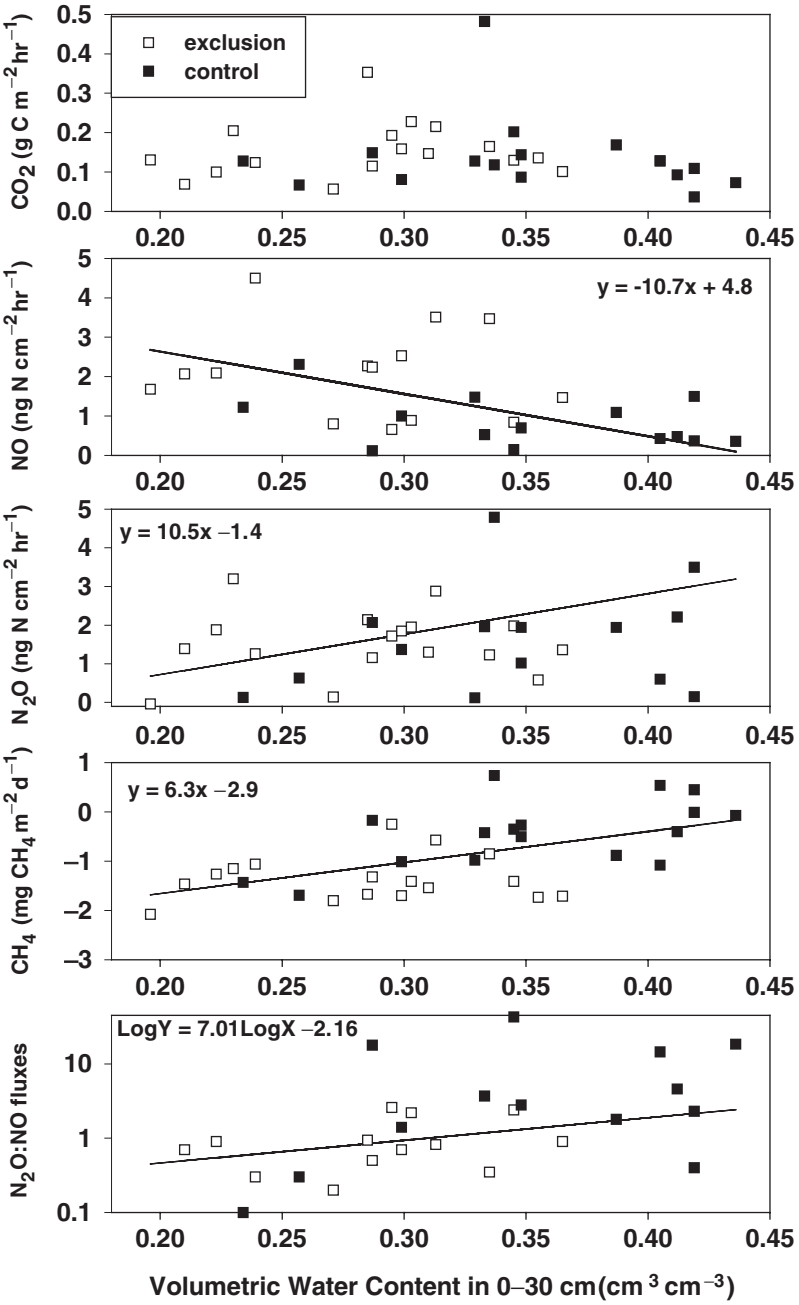

Fig. 2 The relationship between volumetric water content of the top 30 cm soil with surface fluxes of carbon dioxide, nitric oxide, nitrous oxide, methane and the ratio of nitrous oxide/nitric oxide in the throughfall exclusion plot (open symbols) and control plot (solid symbols). The R^2 values for the regression lines are 0.48, 0.15, 0.31, and 0.35 for NO, N_2O, CH_4, and Log(N_2O/NO), respectively. The regression for N_2O is significant at $P<0.05$ and the others are significant at $P<0.01$.

dates of the 13 times that these profiles have been measured so far. The example of pretreatment profiles in December 1999 shows that VWC near the surface was similar in the two plots, but that the exclusion plot had lower initial water content at depth, although error bars often overlap. By the end of the first post-treatment rainy season in July 2000, the exclusion plot had lower water content in the surface horizons, and the differences persisted throughout the remaining sampling dates. By the last shown sampling date in June 2002, differences in VWC were unambiguous at all depths.

The profiles of CO_2 concentrations were remarkably similar in the two plots prior to the exclusion treatment in December 1999. The CO_2 concentrations began

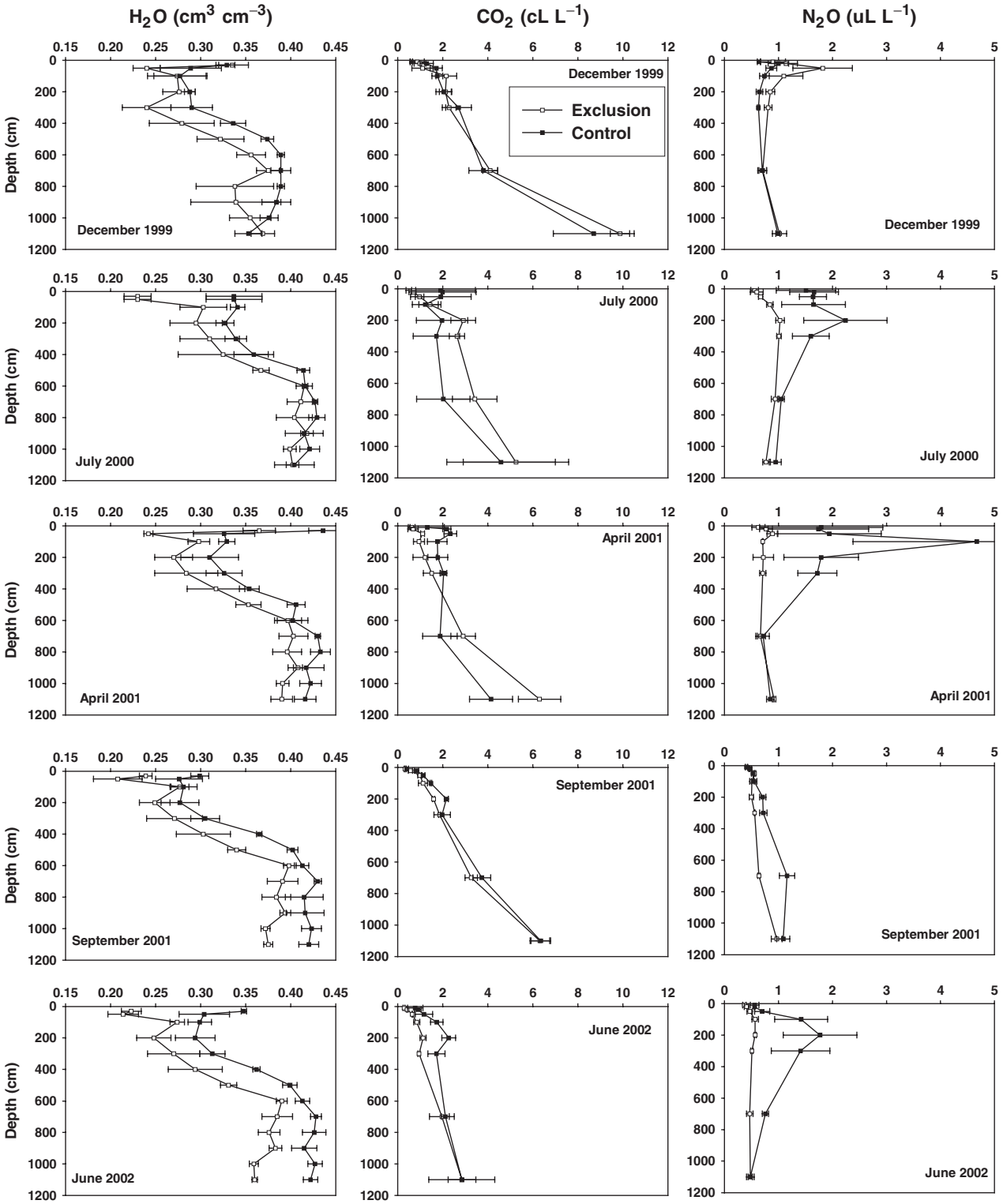

Fig. 3 Depth profiles of volumetric water content, carbon dioxide concentration, and nitrous oxide concentration for five selected dates, including December 1999 (pretreatment dry-to-wet season transition), July 2000 (post-treatment wet-to-dry season transition), April 2001 (wet season), September 2001 (dry season), and June 2002 (end of wet season). Means and standard errors (error bars) are shown for three soil shafts in each of the two plots (open symbols for throughfall exclusion plot and solid symbols for control plot).

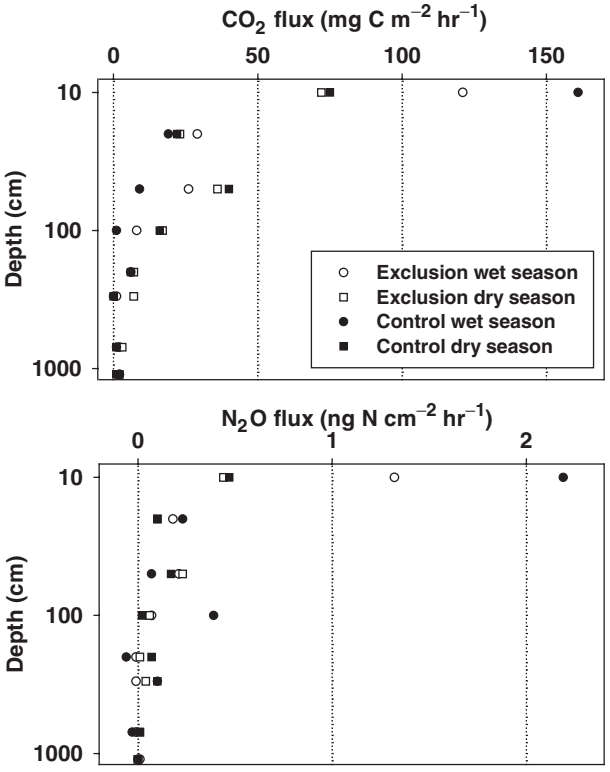

Fig. 4 Fluxes of carbon dioxide and nitrous oxide as a function of depth as calculated by the diffusivity model. Means were calculated across dates within the wet season (circles) and within the dry season (squares) and for the throughfall exclusion plot (open symbols) and control plot (solid symbols). A logarithmic scale is used to distribute the data more evenly along the Y-axis for visual clarity.

diverging in the top 50 cm of soil in 2000 and were higher in the top 200–300 cm in the control plots during subsequent rainy seasons, as in April 2001 and June 2002. Differences were smaller during dry seasons, as in September 2001. The CO_2 concentrations increased with depth in both plots on all dates, indicating at least some CO_2 production as deep as 1100 cm.

The concentrations of N_2O began somewhat higher in the exclusion plot during the December 1999 pretreatment sampling, but this trend quickly reversed during the first post-treatment rainy season. The highest concentration was observed between 50 and 300 cm in control soils during the rainy season. This peak was absent on all dates in the post-treatment exclusion plot and during the dry season (September 2001) in the control plot. Hence, production of N_2O occurred mostly in the top 300 cm of the control plot during the wet season.

Depth profiles of CH_4 are not shown because they showed only one consistent trend at all dates and in both plots – the concentration was usually below ambient (1.8 $\mu L\,L^{-1}$) at all depths, indicating that most of the CH_4 consumption occurred in the top 10 cm. In most cases, the concentrations were $<1.0\,\mu L\,L^{-1}$, and they showed no consistent trend with depth. However, occasional 'hot spots' of CH_4 production were indicated by concentrations of several $\mu L\,L^{-1}$ above ambient at a single depth, but with no recognizable pattern in terms of depth, season, or treatment. The net positive CH_4 fluxes sometimes measured at the surface in the control plots during the wet season (Fig. 1d) were most likely due to such hot spots near the surface directly under a flux chamber, because no consistent gradient of increasing concentration with depth was ever observed in these depth profiles. Hence, no attempt was made to model CH_4 production as a function of depth.

Although the N_2O concentrations peaked at 50–300 cm, the calculated N_2O flux was greatest at 10 cm depth (Fig. 4b) due to a large concentration gradient between that depth and the overlying atmosphere, and because the highest effective diffusivities were calculated for the surface soil. Significantly lower fluxes calculated at 25 cm depth, representing $<20\%$ of the measured surface fluxes, indicate that most of the N_2O production occurred above 25 cm depth. The large peaks of N_2O concentration measured at 50–300 cm in the wet season (Fig. 3) result from modest production and low effective diffusivities at those depths. Consistent with surface flux measurements (Fig. 1b), N_2O fluxes calculated within the profile were higher in the control plot than the exclusion plot and higher in the wet season than in the dry season. Fluxes declined rapidly with increasing depth and were near zero at 700 and 1100 cm. Negative values for calculated fluxes indicate downward diffusion from 200 to 700 cm depths on some dates, particularly in the wet season when production was greatest in the top 300 cm. The increasing N_2O concentration profile with depth observed in the dry season (e.g. September 2001) may be a memory effect of N_2O having diffused to deep horizons during the wet season and not yet having fully diffused back upwards during the dry season. Diffusivities were very low in both seasons in the deep soil (usually 0.001–0.003 cm^3 air cm^{-1} soil s^{-1}).

Calculated fluxes of CO_2 as a function of depth were similar to N_2O, except that all values were positive, indicating at least a small source at all depths (Fig. 4a). During the wet season, the calculated CO_2 flux at 10 cm often equaled or exceeded the mean surface flux due to a very steep concentration gradient between 10 cm and the overlying atmosphere. Much lower fluxes were calculated at 25 cm depth (Fig. 4a). These results indicate that most of the CO_2 production occurred between 10 and 25 cm depth during the wet season, although some production above 10 cm is likely,

suggesting that the diffusion model probably overestimated fluxes at 10 cm.

During the dry season, the calculated flux at 10 cm depth was only about 70% of the surface flux, indicating a significant contribution of production in the 0–10 cm depth increment. It may be that the top 10 cm soil becomes too wet during the wet season for significant aerobic respiration and that respiration increases there as the soils dry during the dry season. This interpretation is consistent with significant production of N_2O and CH_4 in the surface soil from denitrification and methanogenesis in abundant anaerobic microsites of the surface soil during the wet season (Fig. 1c, d). A significant flux of CO_2 is also calculated at 50 and 100 cm depths during the dry season in both plots (Fig. 4a). This result indicates significant CO_2 production (10–20 mg C m^{-2} h^{-1}) down to at least 100 cm, which is consistent with the top 200 cm of soil drying significantly during the dry season (Fig. 3), thus increasing diffusivity, aeration, and perhaps CO_2 production. Interestingly, CO_2 surface fluxes showed less seasonality than the other gases (Fig. 1), which is consistent with aerobic processes being enhanced by some degree of drying and with intermediate soil water contents being optimal for CO_2 production (Linn & Doran, 1984; Fig. 2a).

There appears to be no effect yet observed of throughfall exclusion on CO_2 fluxes, either measured at the surface with chambers (Fig. 1a) or calculated at depth with the diffusivity model (Fig. 4b). It is possible that drought-induced plant stress could reduce root respiration, while fine root mortality enhances microbial decomposition, and these two effects cancel. However, this scenario is still speculative, and, for the moment, we can conclude only that total soil respiration has not been affected by the throughfall exclusion manipulation.

The profiles of total fine root biomass (0–2 mm, live and dead) covaried with the estimates of CO_2 flux as a function of depth calculated for the same months that root biomass was measured (Fig. 5). The roots apparently are the dominant source of CO_2 in deep soil, either directly from root respiration or indirectly from microbial decomposition of root detritus. Although this correlation may not be surprising, we are unaware of any other demonstration of this relationship, because few studies have addressed both root biomass distributions and CO_2 production with soil depth. This covariance lends support that the relative trends of CO_2 flux by depth derived from diffusion model are reliable, although uncertainties remain in the magnitude of these estimates. Moreover, this relationship suggests that we might be able to detect future changes in root distributions and allocation of C belowground as the experiment progresses by continuing to estimate CO_2 production as a function of depth using profiles of diffusivity (as affected by H_2O) and concentrations of CO_2.

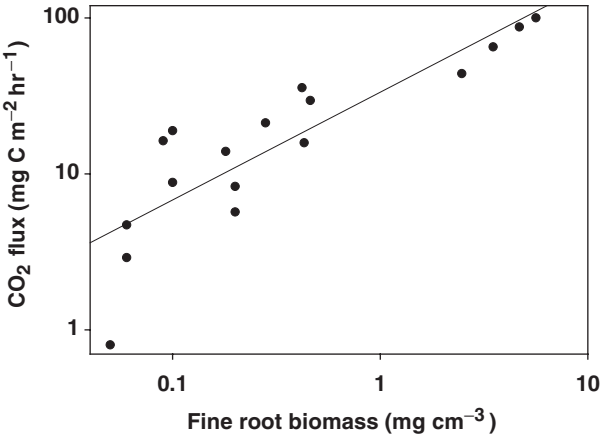

Fig. 5 Relationship between total (live + dead) fine root (0–2 mm diameter) biomass and calculated carbon dioxide flux at 10, 50, 100, 200, 300, and 700 cm depths in exclusion and control plots in August 2000 and July 2001, which are the dates that fine roots were sampled. The regression equation is Log(CO_2 flux) = 0.684 Log(biomass) + 1.52; $R^2 = 0.74$.

Conclusion

This throughfall exclusion experiment has demonstrated that emissions of N_2O and CH_4 from Amazonian forest soils are sensitive to changing climate. The exclusion manipulation, which is similar to the reduction in rainfall experienced during severe El Niño events, lowered annual N_2O emissions by $>40\%$ and increased rates of consumption of atmospheric CH_4 by a factor of >4. No treatment effect has yet been detected for NO and CO_2 fluxes. The responses of these microbial processes after three rainy seasons of the exclusion treatment are characteristic of the anticipated first phase, in which the direct effect of soil aeration on denitrification, methanogenesis, and methanotrophy were observed. A second phase response in which drought-induced plant mortality is followed by increased mineralization of C and N substrates from dead fine roots and by increased foraging of termites on dead coarse roots has not yet been detected. Determining the potential effects of reduced precipitation due to extensive regional land-use change on trace gas processes in Amazonian forest soils will require longer term monitoring of this experiment.

Analyses of depth profiles of N_2O and CO_2 concentrations with a diffusivity model revealed that the top 25 cm soil is the site of most of the wet season

production of N_2O, whereas significant CO_2 production occurs down to 100 cm in both seasons, and small production of CO_2 occurs to at least 1100 cm depth. Covariance of fine root biomass with modeled CO_2 production as a function of depth suggests that trends in belowground C allocation may be inferred from this approach of monitoring and modeling profiles of H_2O and CO_2.

Acknowledgements

This research was supported by grants No. NCC5-332 and No. NCC5-686 of NASA's Terrestrial Ecology Program as part of the Large-scale Biosphere-Atmosphere (LBA) project and by NSF grants DEB 9707556, DEB 0075602 and DEB 0213001. We thank Elizabeth Belk (WHRC) and Renata Tuma Sabá (CNPq DTI Bolsista) for assistance with trace gas measurements, David Ray (WHRC) for assistance with soil water data, E.J. Maklouf Carvalho (Embrapa Amazônia Oriental) for water retention curves, Cláudio J. Reis de Carvalho (Embrapa Amazônia Oriental) for hosting our gas chromatography laboratory, Ricardo Figueiredo and Paulo Moutinho (Embrapa Amazônia Oriental and IPAM) for institutional logistical support, Patrick Crill and Michael Keller (University of New Hampshire) for use of their equipment in Santarém, and CNPq's Programa de Bolsas RHAE for the LBA project for supporting Renata Sabá.

References

Andreae MO, Rosenfeld D, Artaxo P *et al*. (2004) Smoking rain clouds over the Amazon. *Science* (in press).

Cattânio JH, Davidson EA, Nepstad DC *et al*. (2002) Effects of rainfall exclusion on soil emissions of CO_2, CH_4, N_2O, and NO in eastern Amazonia. *Biology and Fertility of Soil*, **36**, 102–108.

Clapperton C (1993) *Quaternary Geology of South America*. Elsevier Science, New York.

Costa MH, Foley JA (2000) Combined effects of deforestation and doubled atmospheric CO_2 concentrations on the climate of Amazonia. *Journal of Climate*, **13**, 18–34.

Davidson EA, Bustamante MMC, Pinto AS (2001) Emissions of nitrous oxide and nitric oxide from soils of native and exotic ecosystems of the Amazon and Cerrado regions of Brazil. In: *Optimizing Nitrogen Management in Food and Energy Production and Environmental Protection: Proceedings of the Second International Nitrogen Conference on Science and Policy* (eds Galloway J, Cowling E, Erisman J, Wisniewski J, Jordan C), pp. 312–319. A.A. Balkema Publishers, Lisse.

Davidson EA, Keller M, Erickson HE *et al*. (2000a) Testing a conceptual model of soil emissions of nitrous and nitric oxides. *Bioscience*, **50**, 667–680.

Davidson EA, Kingerlee W (1997) A global inventory of nitric oxide emissions from soils. *Nutrient Cycling in Agroecosystems*, **48**, 37–50.

Davidson EA, Savage K, Verchot LV *et al*. (2002) Minimizing artifacts and biases in chamber-based measurements of soil respiration. *Agricultural and Forest Meteorology*, **113**, 21–37.

Davidson EA, Schimel JS (1995) Microbial processes of production and consumption of nitric oxide, nitrous oxide and methane. In: *Biogenic Trace Gases: Measuring Emissions from Soil and Water* (eds Matson PA, Harriss RC), pp. 327–357. Blackwell Science, Oxford.

Davidson EA, Trumbore SE (1995) Gas diffusivity and production of CO_2 in deep soils of the eastern Amazon. *Tellus*, **47B**, 550–565.

Davidson EA, Verchot LV (2000) Testing the hole-in-the-pipe model of nitric and nitrous oxide emissions from soils using the TRAGNET database. *Global Biogeochemical Cycles*, **14**, 1035–1043.

Davidson EA, Verchot LV, Cattânio JH *et al*. (2000b) Effects of soil water content on soil respiration in forests and cattle pastures of eastern Amazonia. *Biogeochemistry*, **48**, 53–69.

Dias-Filho M, Davidson EA, Carvalho CJR (2001) Linking biogeochemical cycles to cattle pasture management and sustainability in the Amazon Basin. In: *The Biogeochemistry of the Amazon Basin* (eds McClain ME, Victoria RL, Richey JE), pp. 84–105. Oxford University Press, New York.

Dörr H, Katruff L, Levin I (1993) Soil texture parameterization of the methane uptake in aerated soils. *Chemosphere*, **26**, 697–713.

Fearnside PM (1996) Amazonia and global warming: annual balance of greenhouse gas emissions from land-use change in Brazil's Amazon region. In: *Biomass Burning and Global Change, Vol. 2, Biomass Burning in South America, Southeast Asia, and Temperate and Boreal Ecosystems, and the Oil Fires of Kuwait* (ed. Levine JS), pp. 606–617. MIT Press, Cambridge, MA.

Firestone MK, Davidson EA (1989) Microbiological basis of NO and N_2O production and consumption in soil. In: *Exchange of Trace Gases Between Terrestrial Ecosystems and the Atmosphere* (eds Andreae MO, Schimel DS), pp. 7–21. John Wiley & Sons, New York.

Houghton RA, Lawrence KT, Hackler JL *et al*. (2001) The spatial distribution of forest biomass in the Brazilian Amazon: a comparison of estimates. *Global Change Biology*, **7**, 731–746.

Jipp P, Nepstad DC, Cassel K *et al*. (1998) Deep soil moisture storage and transpiration in forests and pastures of seasonally-dry Amazonia. *Climatic Change*, **39**, 395–412.

Keller M, Reiners WA (1994) Soil-atmosphere exchange of nitrous oxide, nitric oxide, and methane under secondary succession of pasture to forest in the Atlantic lowlands of Costa Rica. *Global Biogeochemical Cycles*, **8**, 399–409.

Kirkman GA, Gut A, Ammann C *et al*. (2002) Surface exchange of nitric oxide, nitrogen dioxide, and ozone at a cattle pasture in Rondônia, Brazil. *Journal of Geophysical Research*, **107**, 8083, doi:10.1029/2001JD000523.

Lammel G, Graßl H (1995) Greenhouse effect of NO_x. *Environmental Science and Pollution Research*, **2**, 40–45.

Linn DM, Doran JW (1984) Effect of water-filled pore space on carbon dioxide and nitrous oxide production in tilled and nontilled soils. *Soil Science Society of America Journal*, **48**, 1267–1272.

Matson PA, Vitousek PM (1990) Ecosystem approach to a global nitrous oxide budget. *Bioscience*, **40**, 667–672.

Matson PA, Vitousek PM, Livingston GP *et al*. (1990) Sources of variation in nitrous oxide from Amazonian ecosystems. *Journal of Geophysical Research*, **95**, 16789–16798.

Moldrup P, Olesen T, Schjønning P *et al*. (2000) Predicting the gas diffusion coefficient in undisturbed soil from soil water

characteristics. *Soil Science Society of America Journal*, **64**, 94–100.

Nepstad DC, Carvalho CJRd, Davidson EA *et al*. (1994) The role of deep roots in the hydrological and carbon cycles of Amazonian forests and pastures. *Nature*, **372**, 666–669.

Nepstad DC, Moutinho PRdS, Dias-Filho MB *et al*. (2002) The effects of rainfall exclusion on canopy processes and biogeochemistry of an Amazon forest. *Journal of Geophysical Research*, **107**, 8085, doi:10.1029/2001JD000360.

Nepstad DC, Uhl C, Pereira CA *et al*. (1996) A comparative study of tree establishment in abandoned pasture and mature forest of eastern Amazonia. *Oikos*, **76**, 25–39.

Nepstad DC, Veríssimo A, Alencar A *et al*. (1999) Large-scale impoverishment of Amazonian forests by logging and fire. *Nature*, **398**, 505–508.

Nobre CA, Sellers PJ, Shukla J (1991) Amazonian deforestation and regional climate change. *Journal of Climate*, **4**, 957–988.

Potter CS, Davidson EA, Verchot LV (1996) Estimation of global biogeochemical controls and seasonality in soil methane consumption. *Chemosphere*, **32**, 2219–2246.

Prather M, Derwent R, Ehhalt D *et al*. (1995) Other trace gases and atmospheric chemistry. In: *Climate Change 1994* (eds Houghton JT, Meira Filho LG, Bruce J, Lee H, Callander BA, Haites E, Harris N, Maskell K), pp. 73–126. Cambridge University Press, Cambridge, UK.

Rosenfeld D (1999) TRMM observed first direct evidence of smoke from forest fires inhibiting rainfall. *Geophysical Research Letters*, **26**, 3105–3108.

Shukla J, Nobre CA, Sellers P (1990) Amazon deforestation and climate change. *Science*, **247**, 1322–1325.

Steudler PA, Melillo JM, Feigl BJ *et al*. (1996) Consequence of forest-to-pasture conversion on CH_4 fluxes in the Brazilian Amazon. *Journal of Geophysical Research*, **101**, 18 547–18 554.

Striegl RG (1993) Diffusional limits to the consumption of atmospheric methane by soils. *Chemosphere*, **26**, 715–720.

Timmermann A, Oberhuber J, Bacher A *et al*. (1999) Increased El Niño frequency in a climate model forced by future greenhouse warming. *Nature*, **395**, 694–697.

Trenberth KE, Hoar TJ (1997) El Niño and climate change. *Geophysical Research Letters*, **24**, 3057–3060.

Verchot LV, Davidson EA, Cattânio JH *et al*. (1999) Land use change and biogeochemical controls of nitrogen oxide emissions from soils in eastern Amazonia. *Global Biogeochemical Cycles*, **13**, 31–46.

Verchot LV, Davidson EA, Cattânio JH *et al*. (2000) Land use change and biogeochemical controls of methane fluxes in soils in eastern Amazonia. *Ecosystems*, **3**, 41–56.

Werth D, Avissar R (2002) The local and global effects of Amazon deforestation. *Journal of Geophysical Research*, **107**, 8087, doi:10.1029/2001JD000717.